



## Scientific-Research Article

# A Fuzzy Fast Terminal Approach for Tracking a Probe Around an Asteroid

Mahsa Azadmanesh<sup>1\*</sup>, Jafar Roshanian<sup>2</sup>, Mostafa Hassanalian<sup>3</sup>

1-2- Department of Aerospace Engineering, K. N. Toosi University of Technology, Tehran, Iran

3- Department of New Mexico University

## ABSTRACT

**Keywords:** FTSMC with the Sign Function, FTSMC with the Saturation Function, Probe Landing, Lyapunov Stability, Fuzzy Control.

*This paper tests the fuzzy system on a previously employed fast terminal sliding mode controller with both the sign and the saturation function to track the landing trajectory of a probe on an asteroid and to further improve the dynamic tracking performance. To make fair judgments on the performance of the suggested method, the proportional derivative sliding mode control with both the sign function and the saturation function is simulated as well. The two-point barycentric gravitational model is used to describe the weak gravity around the asteroid. The proposed fuzzy fast terminal method raises the convergence speed, improves the desired trajectory tracking accuracy and ensures that the system modes are placed on the sliding surface in a short, limited time. The absolute errors for the proportional derivative sliding mode controller, fast terminal sliding mode controller and improved fast terminal sliding mode controller are about 244, 139 and 113. The trajectories along all three coordinate axes in the proportional derivative sliding mode controller, fast terminal sliding mode controller and improved fast terminal sliding mode controller were tracked in 8 seconds, 5 seconds and 4 seconds. The results show how the fuzzy-fast terminal sliding mode control with the saturation function is the better choice of controller and how the fuzzy system is able to adapt to the momentary fluctuations and cover them successfully.*

## Introduction

Asteroids soft-landing needs real time control and adjustment of the trajectory and speed [1]. A novel fuzzy-sliding mode controller is proposed by ref. [2] that achieves the soft-landing trajectory tracking in 2012, while ref. [3] has split the landing control into two parts: the velocity control and the

control over the rate of velocity decline. A strategy for orbital maneuver based on PLO or Piecewise Linear Optimization is proposed and applied on the asteroid soft-landing problem in ref. [4]. Ref. [5] has suggested an autonomous navigation strategy that achieves fast-tracking using the sliding mode variable structure control. A nonlinear optimal control law for moon landing is

1 PhD. Candidate (Corresponding Author) Email: \* mahsa.azadmanesh@yahoo.com

2 Professor

3 Associate Professor

DOI: 10.22034/jast.2022.362213.1131

Submit: 14/09/2022 / Accepted: 31/12/2022

Print ISSN:1735-2134 Online ISSN: 2345-3648

proposed in ref. [6] based on a neuro-fuzzy system. Ref. [7] has employed a fuzzy-variable structure control to guide the final landing trajectory on the moon .

The nonsingular terminal sliding mode control is employed in ref. [8] to be applied to the asteroid soft-landing problem. Ref. [9] suggested a novel algorithm based on nonlinear guidance for a probe that hovers and lands on asteroids .

This study, aims to take the previously employed [10] fast terminal sliding mode control with the sign and the saturation function to track the landing trajectory of a probe on the asteroid 433-Eros and improve the dynamic tracking performance by adding a fuzzy controller. As it is carefully investigated in various papers and dissertations, the fast terminal algorithm seems not to be employed on the asteroid landing problem ever before. Ergo the team decided to check how the system responds to such an approach. The results confirmed the practicality of the method. Then the fuzzy control is added to enhance both fast terminals. In order to be able to make fair judgments on how the suggested methods perform, the proportional derivative sliding mode control with both the sign function and the saturation function is simulated as well. The two-point barycentric gravitational model is used to describe the weak gravity around the asteroid.

**Assumptions**

Table.1 shows the simulation variables and assumptions for the probe landing.

**Table 1.** The simulation variables and assumptions of the probe landing on asteroid EROS433 [5]

Variable		Value	Unit
Optimal Position	Initial	[3200 1300 9000]	m
Optimal Speed	Initial	[-1.2 0.2 -1]	m/s
Landing Position		[2837 928.1 5708]	m
Optimal Speed	Final	[0 0 0]	m/s
Average Asteroid Weight		$6.69 \times 10^5$	kg
Probe Weight		150	kg
Average Asteroid Radius		16000	m
Gravitational Constant		$6.6743 \times 10^{-11}$	$\frac{m^2 kg^{-1}}{s^{-1}}$

**Dynamic Equations in the Fixed-Body Coordinate System**

Fig. 1 shows a schematic view of asteroid 433-Eros. And the probe’s dynamic equations in the fixed-body coordinate system are as follows [1],

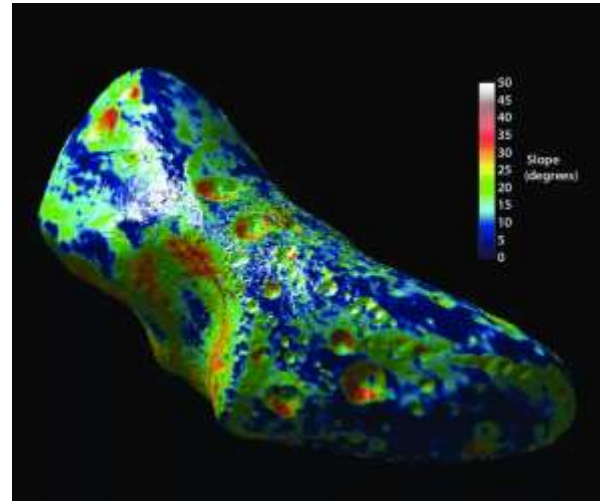


**Fig. 1.** A schematic view of 433-Eros [11].

$$\begin{cases} \ddot{x} - 2\omega\dot{y} - \omega^2x = g_x + u_x + D_x \\ \ddot{y} + 2\omega\dot{x} - \omega^2y = g_y + u_y + D_y \\ \ddot{z} = g_z + u_z + D_z \end{cases} \quad (1)$$

In the dynamic equation  $x$ ,  $y$ , and  $z$  show the probe’s position vector components in the fixed-body coordinate system.  $\omega = 3.3118 \times 10^{-4}$  represents the asteroid angular speed.  $D_x$ ,  $D_y$ , and  $D_z$  represent the modeling uncertainties along each axis. The relative control acceleration vector along the three axes is shown by  $[u_x \ u_y \ u_z]$ . The point gravitation vector with two mass centers along the three axes is shown by  $[g_x \ g_y \ g_z]$  and can be acquired as follows [12],

$$\left\{ \begin{array}{l}
 U = \\
 M_1 \\
 \sqrt{(x-x_1)^2 + (y-y_1)^2 + (z-z_1)^2} + \\
 M_2 \\
 \sqrt{(x-x_2)^2 + (y-y_2)^2 + (z-z_2)^2} \\
 g_x = \frac{\partial U}{\partial x} = \\
 \left( \left( \frac{GM_1(x-x_1)}{((x-x_1)^2 + (y-y_1)^2 + (z-z_1)^2)^{1.5}} + \right. \right. \\
 \left. \left. \frac{GM_2(x-x_2)}{((x-x_2)^2 + (y-y_2)^2 + (z-z_2)^2)^{1.5}} \right) \right) \\
 g_y = \frac{\partial U}{\partial y} = \\
 \left( \left( \frac{GM_1(y-y_1)}{((x-x_1)^2 + (y-y_1)^2 + (z-z_1)^2)^{1.5}} + \right. \right. \\
 \left. \left. \frac{GM_2(y-y_2)}{((x-x_2)^2 + (y-y_2)^2 + (z-z_2)^2)^{1.5}} \right) \right) \\
 g_z = \frac{\partial U}{\partial z} = \\
 \left( \left( \frac{GM_1(z-z_1)}{((x-x_1)^2 + (y-y_1)^2 + (z-z_1)^2)^{1.5}} + \right. \right. \\
 \left. \left. \frac{GM_2(z-z_2)}{((x-x_2)^2 + (y-y_2)^2 + (z-z_2)^2)^{1.5}} \right) \right)
 \end{array} \right. \quad (2)$$

The gravitational potential function of the asteroid is shown by  $U$ , while  $G$  represents the gravitation constant. The two mass points of the asteroid are  $M_1$  and  $M_2$ .  $(x_1, y_1, z_1)$  and  $(x_2, y_2, z_2)$  show the coordinates of the two mass points (Fig. 2).

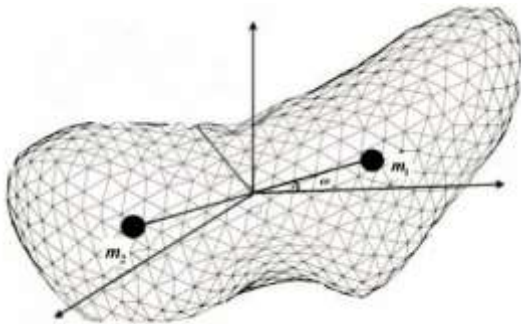


Fig. 2. Mass points of the asteroid EROS433 [12]

### State-Space Equations

State-space equations should be derived as the next step.

$$\left\{ \begin{array}{l}
 X = [x_1 \ x_2 \ x_3 \ x_4 \ x_5 \ x_6]^T = \\
 [x \ \dot{x} \ y \ \dot{y} \ z \ \dot{z}]^T \\
 u = [u_x \ u_y \ u_z]^T
 \end{array} \right. \quad (3)$$

$X$  shows the state-space vector and  $u$  represents control input vectors. The state-space form of Eq. (1) is as follows:

$$\begin{aligned}
 \dot{x}_1 &= x_2 \\
 \dot{x}_2 &= 2\omega x_4 + \omega^2 x_1 + g_x + u_x + D_x \\
 \dot{x}_3 &= x_4 \\
 \dot{x}_4 &= -2\omega x_2 + \omega^2 x_3 + g_y + u_y + D_y \\
 \dot{x}_5 &= x_6 \\
 \dot{x}_6 &= g_z + u_z + D_z
 \end{aligned} \quad (4)$$

### The Fast Terminal Sliding Mode Control Theory

The sliding mode controller keeps the response insensitive to the system's uncertainties and disturbances [13].

The sliding surface for the terminal sliding mode control along the x-axis is as follows:

$$s_1 = \dot{e}_{1x} + \beta(e_{1x})^{\frac{p}{q}} \quad (5)$$

In eq.5  $e_{1x} = x_1 - x_d$  while  $x_d$  shows the trajectory of the optimal landing along the x-direction (Table 1).  $\beta$  is assumed to be a positive parameter.  $p$  and  $q$  ( $p < q$ ) taken to be integers. The nonlinear term,  $(e_{1x})^{p/q}$ , is the reason for a finite time convergence to the origin, which is equal to  $t_s = \left(\frac{p}{\beta(p-q)}\right) |e_1(0)|^{\frac{p-q}{p}}$ . Therefore, parameters  $\beta$ ,  $p$  and  $q$  allow the adjustment of the convergence time.

The abovementioned sliding surface comes with a drawback, and that is the fact that the convergence time strongly relies upon the initial distance of the states from the sliding surface. When this distance is greater, the convergence time increases proportional to  $|e_1(0)|^{\frac{p-q}{p}}$ . The fast terminal sliding mode control is suggested to address this convergence problem, as follows [13-19]:

$$s_1 = \dot{e}_{1x} + \alpha e_{1x} + \beta(e_{1x})^{\frac{p}{q}} \quad (6)$$

In eq. 6  $\alpha$  represents a positive parameter. And adding the extra term to the sliding surface lowers the convergence time significantly. Should the states be on the sliding surface, the equation  $\dot{e}_{1x} = -\alpha e_{1x} - \beta(e_{1x})^{p/q}$  can be established. Whereas when the initial state is in a great distance from the origin, the dynamic will roughly be  $\dot{e}_{1x} = -\alpha e_{1x}$ . On the other hand, when the initial state is very close to the origin, the dynamic would roughly be  $\dot{e}_{1x} = -\beta(e_{1x})^{p/q}$ . By using the parameters  $\alpha$  and  $\beta$ , one can adjust the convergence time for both far and near distances, independently. The equation below obtains the convergence time [14].

$$t_s = \frac{p}{\alpha(p-q)} \left( \ln \left( \alpha e_1^{\frac{p-q}{p}} + \beta \right) - \ln \beta \right) \quad (7)$$

## Control Input Design and Stability Analysis

### Optimal Trajectory Design

The vertical speed should be low enough to keep the probe from being damaged in the safe landing maneuver [1]. Here, a third-degree polynomial, is assumed for the landing trajectory, as described in Eq. (8).

$$x_d(t) = x_0 + x_1 t + x_2 t^2 + x_3 t^3 \quad (8)$$

In order to obtain  $x_0$ ,  $x_1$ ,  $x_2$ , and  $x_3$ , according to Table 1, the following equations are considered.

$$\left. \begin{aligned} x_d(0) &= 3200 \Rightarrow x_0 = 3200 \\ \dot{x}_d(0) &= -1.2 \Rightarrow x_1 = -1.2 \\ x_d(8000) &= 2837 \\ \dot{x}_d(8000) &= 0 \end{aligned} \right\} \quad (9)$$

$$\Rightarrow \begin{cases} x_2 = 2.83 \times 10^{-4} \\ x_3 = -1.73 \times 10^{-8} \end{cases}$$

By considering the final time of  $t = 8000$  sec,  $y$  and  $z$ - axis landing trajectory variables are calculated.

$$\left\{ \begin{aligned} y_d(t) &= 1300 + 0.2t - \\ &6.74 \times 10^{-5}t^2 + 4.58 \times 10^{-9}t^3 \\ z_d(t) &= 9000 - t \\ &+ 9.57 \times 10^{-5}t^2 - 2.76 \times 10^{-9}t^3 \end{aligned} \right. \quad (10)$$

The procedure being similar for all three directions, is why the approach is only explained for the state variable  $x$ . The other directions are calculated in the same way.

### Control Input Design

Taking the simulation parameters values, the position state vectors, as well as the optimal velocities that are listed in Table 1 into consideration, the derivation of Eq. (6) leads to the following equation.

$$\dot{s}_1(x) = \ddot{e}_{1x} + \dot{e}_{1x} \left( \alpha + \beta \frac{p}{q} (e_{1x})^{\frac{p}{q}-1} \right) \quad (11)$$

Knowing the equation of the sliding surface is defined based on the state variables and optimal position, it is expected that the system converges to its optimal position. Hence, the following equation is assumed for the sliding surface.

$$\begin{cases} s_1 = 0 \\ \dot{s}_1 = 0 \end{cases} \quad (12)$$

With respect to the theory of the sliding mode, the control input  $u_x$  is interpreted as [20,21]

$$u_x = u_{xeq} + u_{xs} \quad (13)$$

Here, the parameter  $u_{xeq}$  is the component that holds the states on the defined sliding surface, while  $u_{xs}$  is the switching component that drives those states closer to the sliding surface.,  $u_{xs}$ , as a matter of fact, is the stabilizer of the system, which is determined by assuming the Lyapunov stability.

### The Lyapunov stability

The parameter  $u_{xeq}$  is obtained by setting  $\dot{s}_1 = 0$ .

$$\begin{aligned} \dot{s}_1(x) &= \ddot{e}_{1x} + \dot{e}_{1x} \left( \alpha + \beta \frac{p}{q} (e_{1x})^{\frac{p}{q}-1} \right) = 0 \\ &\Rightarrow (\dot{x}_2 - \dot{x}_{2d}) \\ &+ (x_2 - x_{2d}) \left( \alpha \right. \\ &+ \left. \beta \frac{p}{q} (e_{1x})^{\frac{p}{q}-1} \right) = 0 \\ &\Rightarrow u_{xeq} \\ &= -(2\omega x_4 + \omega^2 x_1 + g_x \\ &+ D_x - \dot{x}_{2d}) \\ &- (x_2 - x_{2d}) \left( \alpha \right. \\ &+ \left. \beta \frac{p}{q} (e_{1x})^{\frac{p}{q}-1} \right) \end{aligned} \quad (14)$$

Assuming the Lyapunov function as a definite positive function:

$$V_1 = \frac{1}{2} s_1^2 > 0 \quad (15)$$

The derivation of Eq. (15) must be a definite negative to assure the asymptotic stability.

$$\begin{aligned}
 \dot{V}_1 &= s_1 \dot{s}_1 = s_1 \left( \ddot{e}_1 \right. \\
 &\quad \left. + \dot{e}_1 \left( \alpha \right. \right. \\
 &\quad \left. \left. + \beta \frac{p}{q} (e_1)^{\frac{p-1}{q}} \right) \right) \\
 &= s_1 \left( (\dot{x}_2 - \dot{x}_2) \right. \\
 &\quad \left. + (x_2 - x_2) \left( \alpha \right. \right. \\
 &\quad \left. \left. + \beta \frac{p}{q} (e_{1x})^{\frac{p-1}{q}} \right) \right) \quad (16) \\
 &= s_1 \left( 2\omega x_4 + \omega^2 x_1 \right. \\
 &\quad \left. + g_x + (u_{xeq} + u_{xs}) \right. \\
 &\quad \left. + D_x - \dot{x}_{2d} \right. \\
 &\quad \left. + (x_2 - x_{2d}) \left( \alpha \right. \right. \\
 &\quad \left. \left. + \beta \frac{p}{q} (e_{1x})^{\frac{p-1}{q}} \right) \right) < 0
 \end{aligned}$$

By substituting Eq. (14) in Eq. (16):

$$\dot{V}_1 = s_1(u_{xs}) < 0 \quad (17)$$

So, a proper candidate for the switching control components that satisfies Eq. (17) would be:

$$u_{xs} = -k_1 \text{sgn}(s_1) \quad (18)$$

Here,  $k_1$  is assumed to be a real positive parameter. By combining the Eqs. (14) and (18), then by substituting the result in Eq. (13), the proposed general equation for tracking the reference trajectory of the probe's is given by Eq. (19).

$$\begin{aligned}
 u_x &= -(2\omega x_4 + \omega^2 x_1 + g_x + D_x \\
 &\quad - \dot{x}_{2d}) \\
 &\quad - (x_2 - x_{2d}) \left( \alpha \right. \\
 &\quad \left. + \beta \frac{p}{q} (e_{1x})^{\frac{p-1}{q}} \right) \\
 &\quad - k_1 \text{sgn}(s_1) \quad (19)
 \end{aligned}$$

### The Fuzzy Control system

We now present a fuzzy method based on [22] which adapts to our system successfully. Sliding mode controllers, as explained before, consist of

two parts: one part is the equivalent control ( $u_{xeq}$ ) while the second part is the switching control ( $u_{xs}$ ). Based on the tasks mentioned for them, (the switching control directs the variables towards the sliding surface, and the equivalent control keeps them on the sliding surface) it can be said that when the system modes are placed at great a distance from the sliding surface, the switching control's role is more important. On the other hand, when the system modes are closer to the sliding surface, the equivalent control's effect is greater. So, the fuzzy coefficients can be put as follows:

$$u_x = au_{xeq} + bu_{xs} \quad (20)$$

The coefficients a and b change between 0 and 1. Should the system modes be far from the sliding surface, a = 0 and b = 1 are assumed, and should they be on the sliding surface, a = 1 and b = 0 are considered. The coefficients vary between zero and one in other conditions. The distance length between the states and the sliding surface is put as follows.

$$D_i = \frac{c_{1i}x_1 + c_{2i}x_2 + \dots + c_{ni}x_n}{\sqrt{c_{1i}^2 + c_{2i}^2 + \dots + c_{ni}^2}} \quad (21)$$

The number of system inputs is shown by m:

$$D = \sqrt{\sum_{i=1}^m D_i^2} \quad (22)$$

Based on where D is placed, the coefficients are assigned to the parameters a and b. They may also be assumed as continuous values as follows [22]:

$$\begin{cases} a(D) = e^{-ND} \\ b(D) = 1 - e^{-MD} \end{cases} \quad (22)$$

Where parameters M and N are assumed to be arbitrary coefficients which determine the ascent and descent rate of the coefficients a and b.

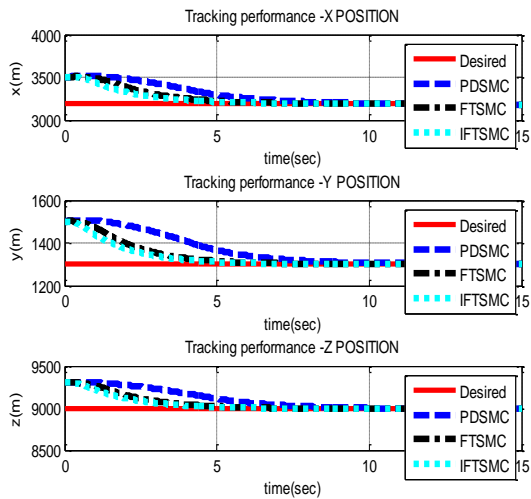
In this paper two fuzzy fast terminal sliding mode controllers are employed and evaluated. At first, in the switching input, the sign function is adopted, then, the it is replaced by a saturation function.

### MATLAB Simulations

#### Fast Terminal Sliding Mode Control with a Sign Function

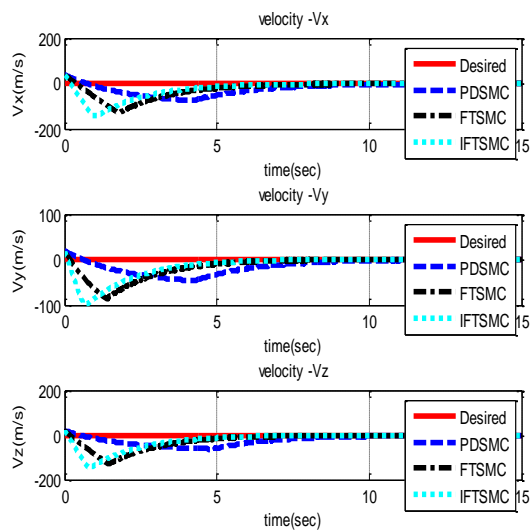
By considering the simulation time to be 15 seconds, the sampling time to be 0.01 of a second,

and by referring to Table 1, the control inputs were implemented for all three directions, and the following figures were derived.



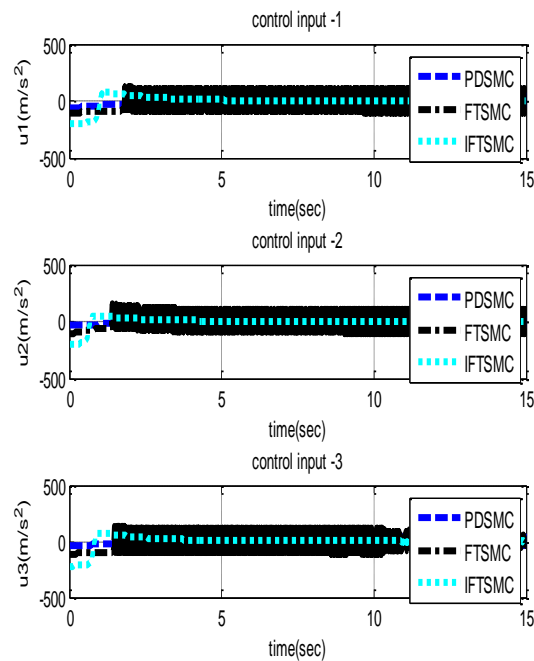
**Fig. 3.** The tracking performance of the desired probe trajectory with a classic PD sliding mode, fast terminal mode and improved fast terminal with a sign function

Fig. 3 shows how the improved fast terminal is able to track the optimal trajectory in a shorter period than both the classic proportional derivative sliding mode control and the fast terminal control.



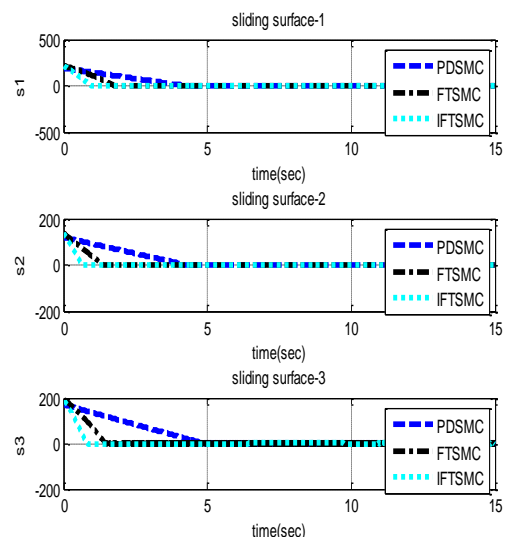
**Fig. 4.** The probe optimal velocity tracking with a classic PD sliding mode, fast terminal mode and improved fast terminal mode with a sign function

Fig. 4 shows how the improved fast terminal sliding mode controller is able to track the optimal probe speed faster than the classic proportional derivative sliding mode controller and the fast terminal sliding mode controller.



**Fig. 5.** The control attempt with a classic PD sliding mode, fast terminal mode and improved fast terminal mode with a sign function

A notably large amount of chattering or parasitic oscillation is illustrated in Fig. 5. The chattering happens in the control inputs in both the proportional derivative sliding mode and the fast terminal one. Nevertheless, the fluctuations are efficiently eliminated by the fuzzy system, indicating that the fuzzy control adapts to the momentary changes well enough.



**Fig. 6.** Sliding surface to control with a classic PD sliding mode, fast terminal mode and improved fast terminal mode with a sign function

In Fig. 6 it is shown how the Improved fast terminal sliding mode controller is able to

converge to the sliding surface much faster than the proportional derivative sliding mode controller and the fast terminal sliding mode one.

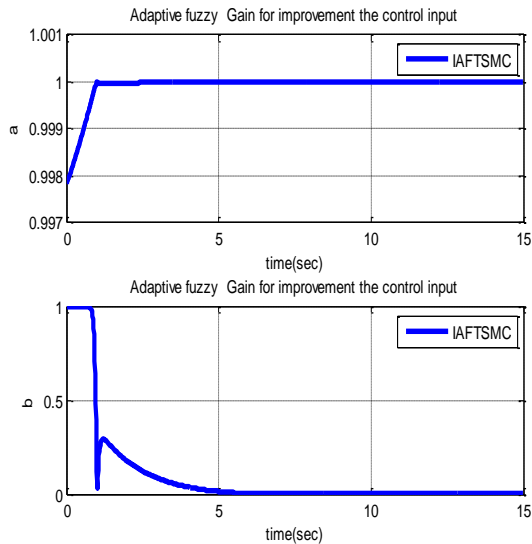


Fig. 7. The adaptive coefficients of the improved fast terminal sliding mode control system.

Fig. 7 illustrates the fuzzy adaptive coefficients responsible for the elimination of the chattering phenomenon and the behavior improvement of the control inputs as well as the system response speed increase. In the beginning, where it is required to direct the state variables towards the sliding surface, the coefficient  $b = 1$  is assumed, and when the state variables are placed on the sliding surface, the coefficient  $a$  is activated to lower the effect of the coefficient  $b$ , so that the state variables are maintained on the sliding surface, based on Eq. (20).

The assessment of Figs. 4-6, revealed that the trajectories along all three coordinate axes in the proportional derivative sliding mode controller, fast terminal sliding mode controller and improved fast terminal sliding mode controller were tracked in 8 seconds, 5 seconds and less than 4 seconds.

### Fast Terminal Sliding Mode Control with a Hyperbolic Tangent Function

By considering the simulation time to be 15 seconds, the sampling time to be 0.01 of a second, and by referring to Table 1, the control inputs were implemented for all three directions, and the following figures were derived.

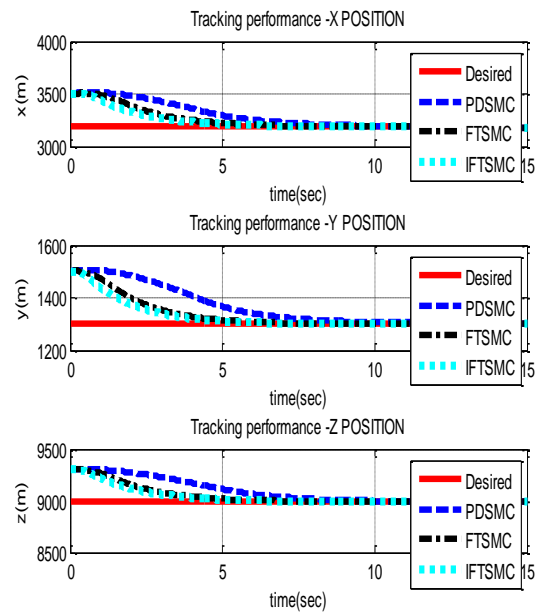
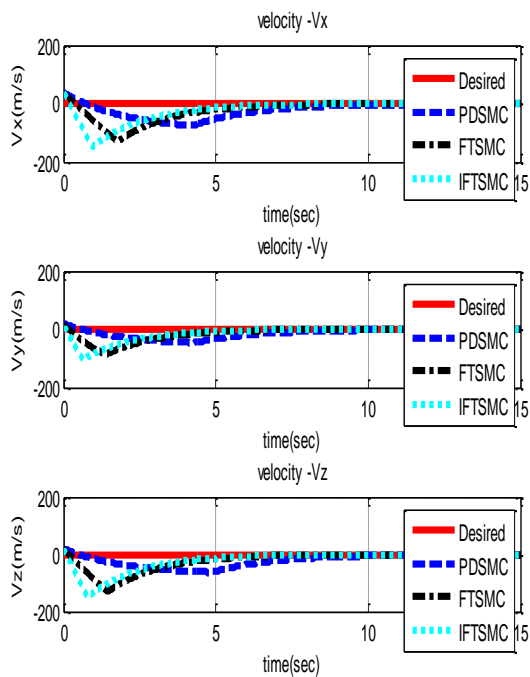
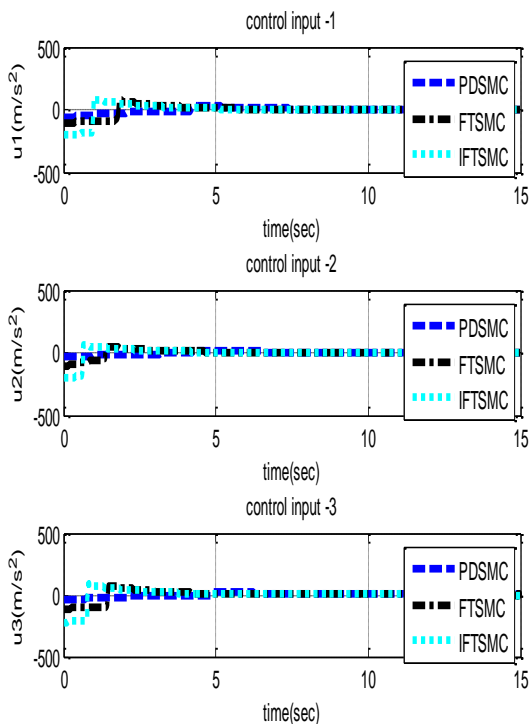


Fig. 8. Tracking the desired trajectory of the probe with classic PD sliding mode, fast terminal mode and improved fast terminal mode with a hyperbolic tangent function

Fig. 8, shows that tracking the desired path by the fast terminal sliding mode control improved with the fuzzy system is done faster than the other two controllers. Also, in Fig. 9, it is well illustrated that tracking the optimal speed of the spacecraft by fast terminal sliding mode control improved with the fuzzy system is done in a shorter time than PDSMC and FTSMC. Fig. 10, shows that due to the use of the hyperbolic tangent saturation function, chattering is efficiently eliminated, while the performance of tracking the optimal trajectory of the probe by the improved FTSMC is enhanced, as the tracking is performed more rapidly than PDSMC and FTSMC.



**Fig. 9.** Tracking the optimal trajectory of the probe with classic PD sliding mode, fast terminal mode and improved fast terminal mode with a hyperbolic tangent function



**Fig. 10.** The control attempt with PDCMC, FTSMC and improved FTSMC modes with a hyperbolic tangent function

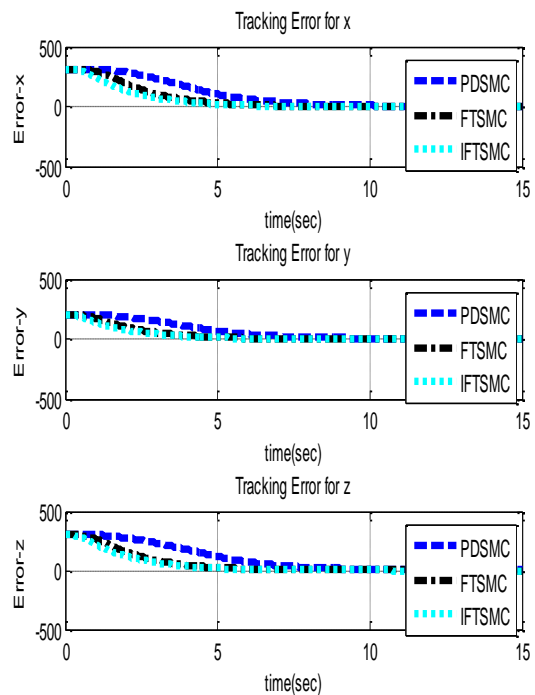


**Fig. 11.** Location tracking error for three moving axes PDCMC, FTSMC and improved FTSMC modes with a hyperbolic tangent function

Figs. 8-10 show that the trajectory tracking was achieved more smoothly due to the inherent characteristics of saturation functions such as hyperbolic tangent. Hence, the oscillations of states and input control were eliminated in Fig. 10. As illustrated in Fig. 10, the position tracking error tended to become zero, while the tracking had an efficient accuracy, with improved FTSMC being more accurate than FTSMC and the classic PD sliding mode.

Table 2 reports the total error for the controllers.

**Table 2.** The absolute error for improved FTSMC, FTSMC and PD sliding mode controller.

Controller	Value
Improved Fast Terminal Sliding Mode Controller	113/4074
Fast Terminal Sliding Mode Controller	139/6112
Proportional-Derivative Sliding Mode Controller	244/8155

Obviously the absolute error value for the Improved Fast Terminal Sliding Mode Controller was significantly lower than the other two.

Fig. 12 illustrates a 3D landing trajectory of the probe from the beginning ( $t = 0$ ) to the end ( $t =$

8000 s), based on the optimal trajectory tracking. The tracking was done fast and accurate. And the Improved Fast Terminal Sliding Mode Controller outperformed the other two.

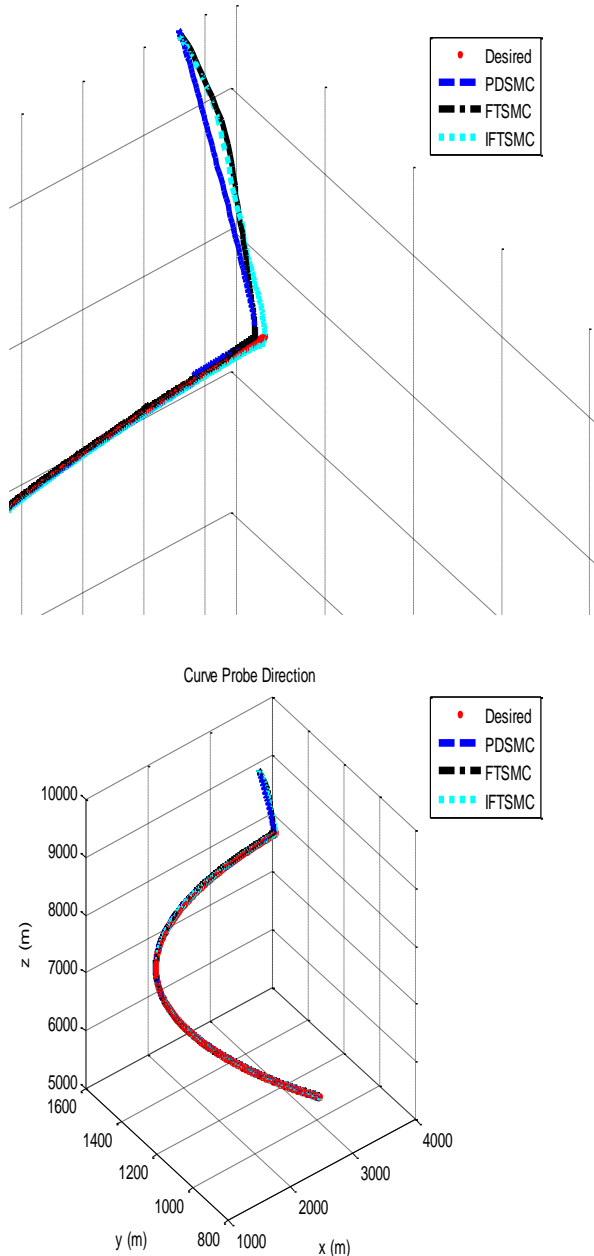


**Fig. 12.** Location tracking error for three moving axes with improved FTSMC, FTSMC and PDCMC modes with a hyperbolic tangent function

The results show how the chattering affects the states' derivatives. Regarding the Fourier transformation as follows [20,21],

$$\frac{d}{dt}x(t) \overset{F}{\leftrightarrow} j\omega X(j\omega) \quad (23)$$

Eq. (23) shows that the linear amplification of system frequencies results in time derivation, which means that higher frequencies are amplified and lower frequencies do not experience much change.

### Conclusions

This paper employed the fuzzy fast terminal sliding mode control with the sign and the saturation function with the purpose of landing a probe on the asteroid 433-Eros. Sliding mode controllers are one of the most common controllers for nonlinear systems, because of their relative simplicity and their high resistance to uncertainties and perturbations. However, they experience a lot of chattering especially in rapid dynamics systems. The sign function is replaced by a saturation function to make the behavior smoother while reducing the oscillations. The proposed fuzzy fast terminal method raised the convergence speed, improved the desired trajectory tracking accuracy and ensured that the system modes are placed on the sliding surface in a short, limited time. The absolute errors for the proportional derivative sliding mode controller, fast terminal sliding mode controller and improved fast terminal sliding mode controller were about 244, 139 and 113. Minimum error belonged to the improve fast terminal sliding mode controller. The trajectories along all three coordinate axes in the proportional derivative sliding mode controller, fast terminal sliding mode controller and improved fast terminal sliding mode controller were tracked in 8 seconds, 5 seconds and 4 seconds. The results show how the fuzzy-fast terminal sliding mode control with the saturation function is the better choice of controller. Finally, it is worthy of mention that the improved fast-terminal sliding mode control method is a new and efficient method in the space industry and can be implemented on similar systems.

### References

- [1] Li, Yuanchun, He Wang, Bo Zhao, and Keping Liu. "Adaptive fuzzy sliding mode control for the probe soft landing on the asteroids with weak gravitational field." *Mathematical Problems in Engineering* 2015 (2015). <https://doi.org/10.1155/2015/582948>
- [2] Yang, Yue-neng, Jie Wu, and Wei Zheng. "Trajectory tracking for an autonomous airship using fuzzy adaptive sliding mode control." *Journal of Zhejiang University SCIENCE C* 13, no. 7 (2012): 534-543. <https://doi.org/10.1631/jzus.C1100371>
- [3] Cui, H. T., X. Y. Shi, and P. Y. Cui. "Guidance and control law for soft landing asteroid." *Journal of Flight Dynamics*

- 20 (2002): 35-38. <https://doi.org/10.15982/j.issn.2095-7777.2019.02.010>
- [4] Hao, Zhao, Chen, and Zhan, "Orbital maneuver strategy design based on piecewise linear optimization for spacecraft soft landing on irregular asteroids", Chinese Journal of Aeronautics, Vol. 20, No. 33 PP.2694–2706, 2020.
- [5] Cui, P. Y., S. Y. Zhu, and H. T. Cui. "Autonomous impulse maneuver control method for soft landing on small bodies." *Journal of Astronautics* 29, no. 2 (2008): 511-516. <https://doi.org/10.15982/j.issn.2095-7777.2019.02.010>
- [6] Zexu, Zhang, Wang Weidong, Li Litao, Huang Xiangyu, Cui Hutao, Li Shuang, and Cui Pingyuan. "Robust sliding mode guidance and control for soft landing on small bodies." *Journal of the Franklin Institute* 349, no. 2 (2012): 493-509. <https://doi.org/10.1016/j.jfranklin.2011.07.007>
- [7] Carson, John, Behcet Acikmese, Richard Murray, and Douglas MacMynowski. "Robust model predictive control with a safety mode: applied to small-body proximity operations." In *AIAA Guidance, Navigation and Control Conference and Exhibit*, p. 7243. 2008. <https://doi.org/10.2514/6.2008-7243>
- [8] Lan, Qixun, Shihua Li, Jun Yang, and Lei Guo. "Finite-time soft landing on asteroids using nonsingular terminal sliding mode control." *Transactions of the Institute of Measurement and Control* 36, no. 2 (2014): 216-223. <https://doi.org/10.1177%2F0142331213495040>
- [9] Yang, Hongwei, Xiaoli Bai, and Hexi Baoyin. "Finite-time control for asteroid hovering and landing via terminal sliding-mode guidance." *Acta Astronautica* 132 (2017): 78-89. <https://doi.org/10.1016/j.actaastro.2016.12.012>
- [10] Azadmanesh, M., Roshanian, J., & Hassanalian, M. (2023). Fast Terminal Sliding Mode control for the soft Landing of a space Robot on an Barycentric Gravitational Model. *Journal of Aerospace Science and Technology*, 16(1).
- [11] Jewitt, David, Jane Luu, and Chadwick Trujillo. "Large Kuiper belt objects: the Mauna Kea 8K CCD survey." *The Astronomical Journal* 115.5 (1998): 2125.
- [11] Shornikov, Andrei, and Olga Starinova. "Simulation of controlled motion in an irregular gravitational field for an electric propulsion spacecraft." In *2015 7th International Conference on Recent Advances in Space Technologies (RAST)*, pp. 771-776. IEEE, 2015. <https://doi.org/10.1109/RAST.2015.7208444>
- [12] Shornikov, Andrey, and Olga Starinova. "Boundary problem solution algorithm for the task of controlled spacecraft motion in irregular gravitational field of an asteroid." *Procedia engineering* 185 (2017): 411-417. <https://doi.org/10.1016/j.proeng.2017.03.323>
- [13] Ebrahimi, Behrouz, Mohsen Bahrami, and Jafar Roshanian. "Optimal sliding-mode guidance with terminal velocity constraint for fixed-interval propulsive maneuvers." *Acta Astronautica* 62.10-11 (2008): 556-562.
- [14] Yu, Xinghuo, and Man Zhihong. "Fast terminal sliding-mode control design for nonlinear dynamical systems." *IEEE Transactions on Circuits and Systems I: Fundamental Theory and Applications* 49, no. 2 (2002): 261-264. <https://doi.org/10.1109/81.983876>
- [15] Mobayen, Saleh, and Fairouz Tchier. "Nonsingular fast terminal sliding-mode stabilizer for a class of uncertain nonlinear systems based on disturbance observer." *Scientia Iranica* 24, no. 3 (2017): 1410-1418. <https://dx.doi.org/10.24200/sci.2017.4123>
- [16] Shuang, Li, and Cui Pingyuan. "Landmark tracking based autonomous navigation schemes for landing spacecraft on asteroids." *Acta Astronautica* 62, no. 6-7 (2008): 391-403. <https://doi.org/10.1016/j.actaastro.2007.11.009>
- [17] Furfaro, Roberto, Dario Cersosimo, and Daniel R. Wibben. "Asteroid precision landing via multiple sliding surfaces guidance techniques." *Journal of Guidance, Control, and Dynamics* 36, no. 4 (2013): 1075-1092. <https://doi.org/10.2514/1.58246>
- [18] Gui, Haichao, and Anton HJ de Ruiter. "Control of asteroid-hovering spacecraft with disturbance rejection using position-only measurements." *Journal of Guidance, Control, and Dynamics* 40, no. 10 (2017): 2401-2416. <https://doi.org/10.2514/1.G002617>
- [19] Kasaeian, Seyed Aliakbar, and Masoud Ebrahimi. "Robust Switching Surfaces Sliding Mode Guidance for Terminal Rendezvous in Near Circular Orbit." *Journal of Space Science and Technology* 11, no. 2 (2018): 21-31.
- [20] Perruquetti, Wilfrid, and Jean Pierre Barbot, eds. *Sliding mode control in engineering*. Vol. 11. New York: Marcel Dekker, 2002.
- [21] Azar, Ahmad Taher, and Quanmin Zhu, eds. *Advances and applications in sliding mode control systems*. Cham: Springer International Publishing, 2015.
- [22] Bathaee, and M. Jafari Harandi, "Decentralized Load Frequency Control of Multi-Area Power Systems Using Combined Variable Structure and Fuzzy Logic Controller", *IFAC Artificial Intelligence in Real-Time Control*, Kuala Lumpur, Malaysia, 1997.

## COPYRIGHTS

©2023 by the authors. Published by Iranian Aerospace Society This article is an open access article distributed under the terms and conditions of the Creative Commons Attribution 4.0 International (CC BY 4.0) (<https://creativecommons.org/licenses/by/4.0/>).

